ASTER DEM Performance

Hiroyuki Fujisada, G. Bryan Bailey, Glenn G. Kelly, Seiichi Hara, and Michael J. Abrams

***Abstract*—The Advanced Spaceborne Thermal Emission and Reflection Radiometer (ASTER) instrument onboard the National Aeronautics and Space Administration's Terra spacecraft has an along-track stereoscopic capability using its a near-infrared spectral band to acquire the stereo data. ASTER has two telescopes, one for nadir-viewing and another for backward-viewing, with a base-to-height ratio of 0.6. The spatial resolution is 15 m in the horizontal plane. Parameters such as the line-of-sight vectors and the pointing axis were adjusted during the initial operation period to generate Level-1 data products with a high-quality stereo system performance. The evaluation of the digital elevation model (DEM) data was carried out both by Japanese and U.S. science teams separately using different DEM generation software and reference databases. The vertical accuracy of the DEM data generated from the Level-1A data is 20 m with 95% confidence without ground control point (GCP) correction for individual scenes. Geolocation accuracy that is important for the DEM datasets is better than 50 m. This appears to be limited by the spacecraft position accuracy. In addition, a slight increase in accuracy is observed by using GCPs to generate the stereo data.**

***Index Terms*—Advanced Spaceborne Thermal Emission and Reflection Radiometer (ASTER) instrument, digital elevation model (DEM), high resolution, optical sensor, stereo.**

I. Introduction

THE Advanced Spaceborne Thermal Emission and Reflection Radiometer (ASTER) is an advanced multispectral imager that was launched onboard the Terra spacecraft in December 1999. ASTER covers a wide spectral region with 14 bands from visible to thermal infrared with high spatial, spectral, and radiometric resolution. The wide spectral region is covered by three separate telescopes. Three visible and near-infrared (VNIR) bands, six shortwave infrared (SWIR) bands, and five thermal infrared (TIR) bands have a spatial resolution of 15, 30, and 90 m, respectively. An additional telescope is used to see backward in the VNIR spectral band (band 3B) for stereoscopic capability that is the major subject of this paper. The spectral passbands of ASTER are shown in Table I.

The Terra spacecraft is in a circular, nearly polar orbit at an altitude of 705 km. The orbit is Sun-synchronous with a local equatorial crossing time of 10:30 A.M., returning to the same orbit every 16 days. More details on the ASTER instrument and its science objectives are described in another paper [1].

Manuscript received October 24, 2004; revised March 4, 2005.

H. Fujisada is with the Sensor Information Laboratory Corporation, Ibaraki 305-0005, Japan.

G. B. Bailey is with the Earth Resources Observations Systems Data Center, U.S. Geological Survey, Sioux Falls, SD 57198 USA.

G. G. Kelly was with the Earth Resources Observations Systems Data Center, U.S. Geological Survey, Sioux Falls, SD 57198 USA. He is now retired.

S. Hara is with the Central Computer Service Co., Ltd., Tokyo 105-0001, Japan.

M. J. Abrams is with Jet Propulsion Laboratory, California Institute of Technology, Pasadena, CA 91109 USA.

Digital Object Identifier 10.1109/TGRS.2005.847924

TABLE I
SPECTRAL PASSBAND

Subsystem	Band No.	Spectral Range (μm)	Spatial Resolution
VNIR	1	0.52 - 0.60	15 m
	2	0.63 - 0.69	
	3N	0.78 - 0.86	
	3B	0.78 - 0.86	
SWIR	4	1.600 - 1.700	30 m
	5	2.145 - 2.185	
	6	2.185 - 2.225	
	7	2.235 - 2.285	
	8	2.295 - 2.365	
	9	2.360 - 2.430	
TIR	10	8.125 - 8.475	90 m
	11	8.475 - 8.825	
	12	8.925 - 9.275	
	13	10.25 - 10.95	
	14	10.95 - 11.65	

The ASTER instrument produces two types of Level-1 data, Level-1A and Level-1B. Level-1A data are formally defined as reconstructed, unprocessed instrument data at full resolution [2]. According to this definition the ASTER Level-1A data consist of the image data, the radiometric coefficients, the geometric coefficients, and other auxiliary data without applying the coefficients to the image. The Level-1B data are generated by applying these coefficients for radiometric calibration and geometric resampling. The Level-1A data are used as source data to generate digital elevation model (DEM) products, because many useful instrument geometric parameters and the spacecraft information are included in them. These parameters are available to generate high-quality DEM data products without ground control point (GCP) correction for individual scenes.

The instrument geometric parameters, such as the line-of-sight (LOS) vectors and the pointing axis vectors were precisely adjusted through the validation activity using many GCPs [3], [4]. The DEM data, which are processed only by these system parameters, were demonstrated to have excellent accuracy. The evaluation of the DEM data was carried out both by Japanese and U.S. science teams separately using different DEM generation software and reference databases.

II. Stereo System Design

The VNIR subsystem has two telescopes, a nadir-looking telescope and a backward-looking telescope. Fig. 1 shows the VNIR configuration. The relation between base-to-height (B/H) ratio and α is $\mathrm{B/H} = \tan\alpha$, where α is the angle between the nadir and the backward direction at a point on the Earth's surface. The angle α, which corresponds to B/H ratio of 0.6, is 30.96°. By considering the curvature of the Earth's surface, the setting angle between the nadir and the backward telescope was designed to be 27.60°.

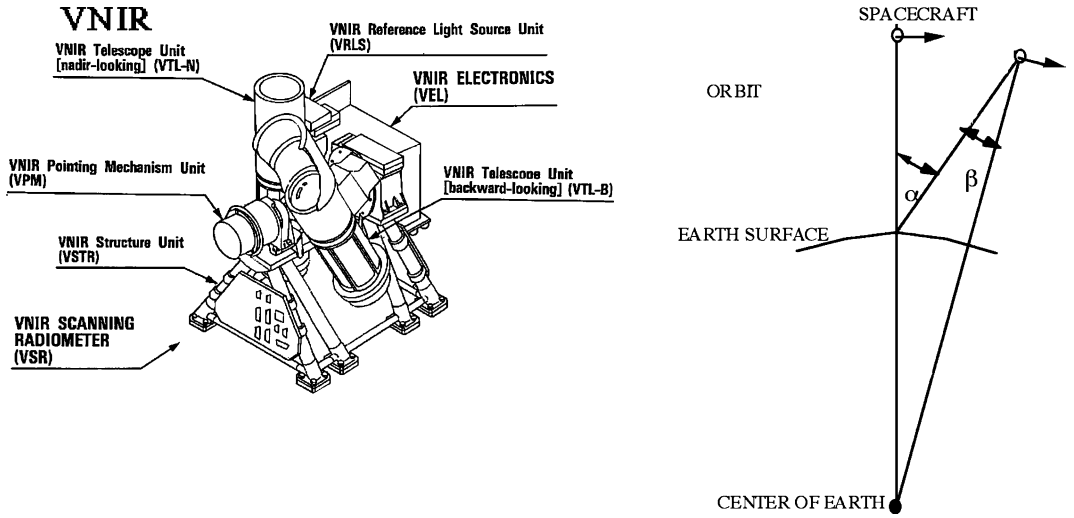

Fig. 1. VNIR configuration.

The pointing function is provided for global coverage in the cross-track direction, since the swath width of ASTER is 60 km and the distance between the neighboring orbits is 172 km at the equator. The optical axes of the nadir and backward telescopes can be tilted simultaneously in the cross-track direction to cover a wider range.

III. Calibration of Stereo Parameters

The DEM data are composed of two horizontal components (latitude and longitude) and one vertical component (elevation). Three instrument parameters are important for precise DEM generation: 1) LOS vectors of bands 3N and band 3B; 2) VNIR pointing axis vector; and 3) encoder value for cross-track pointing angle. The horizontal components can be corrected by an adjustment of the band 3N LOS vectors, the pointing axis vector (unit vector along the cross-track pointing axis), and the encoder to minimize the geolocation errors. The vertical component can be corrected by an adjustment of the band 3B LOS vectors to minimize the elevation errors.

For the VNIR bands, the x, y, and z components of the LOS vectors can be expressed by a fourth-order polynomial on the detector number j_m

$$\begin{aligned} S_{mx}(j_m) &= K_{mx0} + K_{mx1} j_m + K_{mx2} j_m^2 + K_{mx3} j_m^3 + K_{mx4} j_m^4 \\ S_{my}(j_m) &= K_{my0} + K_{my1} j_m + K_{my2} j_m^2 + K_{my3} j_m^3 + K_{my4} j_m^4 \\ S_{mz}(j_m) &= K_{mz0} + K_{mz1} j_m + K_{mz2} j_m^2 + K_{mz3} j_m^3 + K_{mz4} j_m^4. \end{aligned} \tag{1}$$

The suffix m is the band number (i.e., 1, 2, 3N, and 3B for VNIR). The LOS vector of each detector is defined for the nadir pointing position toward the navigation base reference (NBR) of the spacecraft. The initial LOS vectors and the pointing axis vector were evaluated on the ground in the preflight phase. Since the preflight evaluation accuracy is not sufficient for precise DEM generation, parameter calibration was carried out during the initial checkout period using many GCPs prepared for the geometric validation activity.

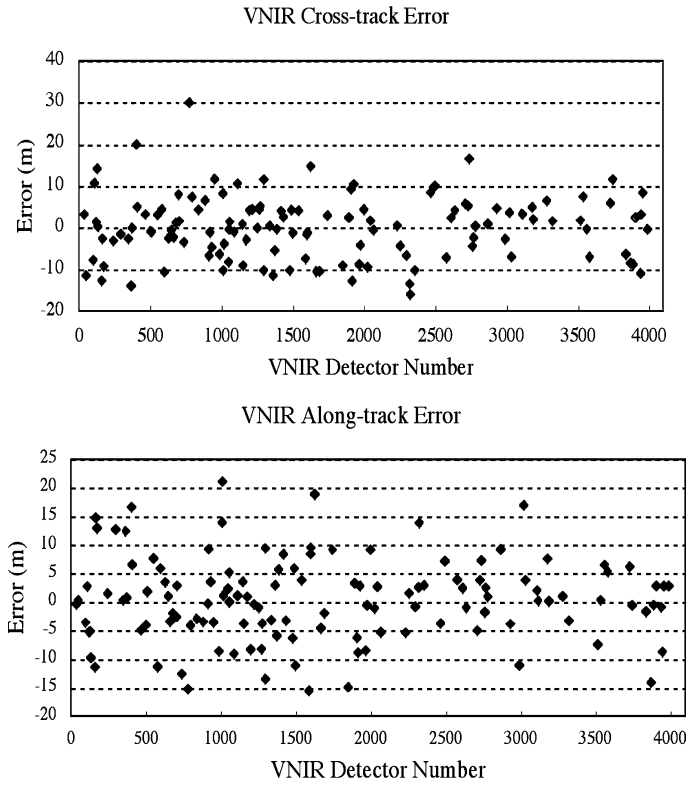

Fig. 2. Band 3N LOS vector calibration accuracy.

A. Band 3N LOS Vector Calibration

For geolocation error evaluation, 127 GCPs were prepared over virtually the entire cross-track area for an image acquired with nearly zero cross-track pointing. The LOS vector coefficients in (1) were corrected from a set of cross-track and along-track errors. The geolocation error analysis was carried out again for the updated Level-1 image processed using corrected LOS vectors to confirm the calibration accuracy as shown in Fig. 2. The error dispersion was caused mainly by the individual GCP errors. The results in Fig. 2 indicate that

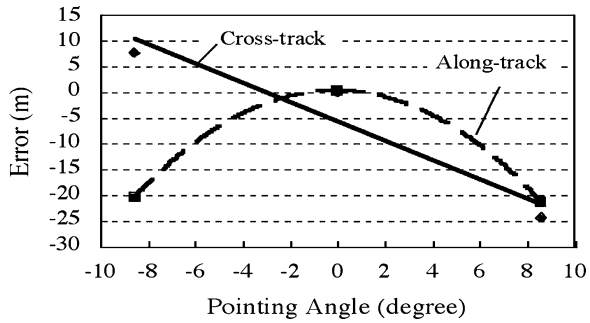

Fig. 3. Pointing angle dependence of LOS vector calibration.

the image distortion in one scene is roughly less than one pixel (15 m).

B. Pointing Axis and Encoder Calibration

Geolocation error evaluation for pointing angles of $+8.59°$ and $-8.58°$ was carried out using 10 and 22 GCPs, respectively. For an observation with a large cross-track pointing, the pointing axis error and the encoder error are responsible for the along-track and the cross-track geolocation errors, respectively. These instrument parameters were corrected to minimize the geolocation errors. Fig. 3 shows the residual geolocation errors after these parameter corrections. The spacecraft position error for each observation is mainly responsible for the residual errors.

C. Band 3B LOS Vector Calibration

The LOS vector adjustment of the band 3B was carried out by comparing the elevation data of the DEM product with the existing DEM database. The LOS vectors of the band 3B can be expressed by the fourth-order polynomial on the detector number j_m as shown in (1). The correction procedure is the same as in the case of band 3N. The Level-1A image acquired by the nadir pointing setting was used to evaluate the elevation errors and then correct the LOS vectors of the band 3B. The elevation data generated using the Level-1A image acquired by the $\pm 8.55°$ cross-track pointing were used to confirm the elevation accuracy for a large pointing angle.

Plain areas with a low elevation were selected for the LOS vector correction. The Kanto plain, which includes Tokyo metropolitan area, is one of the best areas for this purpose. Fig. 4 shows the residual elevation errors for three pointing settings and indicates that the elevation errors due to the corrected instrument system parameters are roughly less than 10 m.

IV. ASTER DEM Data Products—Japanese Version

The Japanese version of the ASTER DEM data product is produced by the ASTER Ground Data System (ASTER GDS) at the Earth Remote Sensing Data Analysis Center (ERSDAC) in Japan using specially developed DEM software. The basic concept of the algorithm developed is to generate DEM data using the instrument and the spacecraft ephemeris parameters only without referring to ground control points for individual scenes. This process is carried out as follows.

1) Input the Level-1A data.

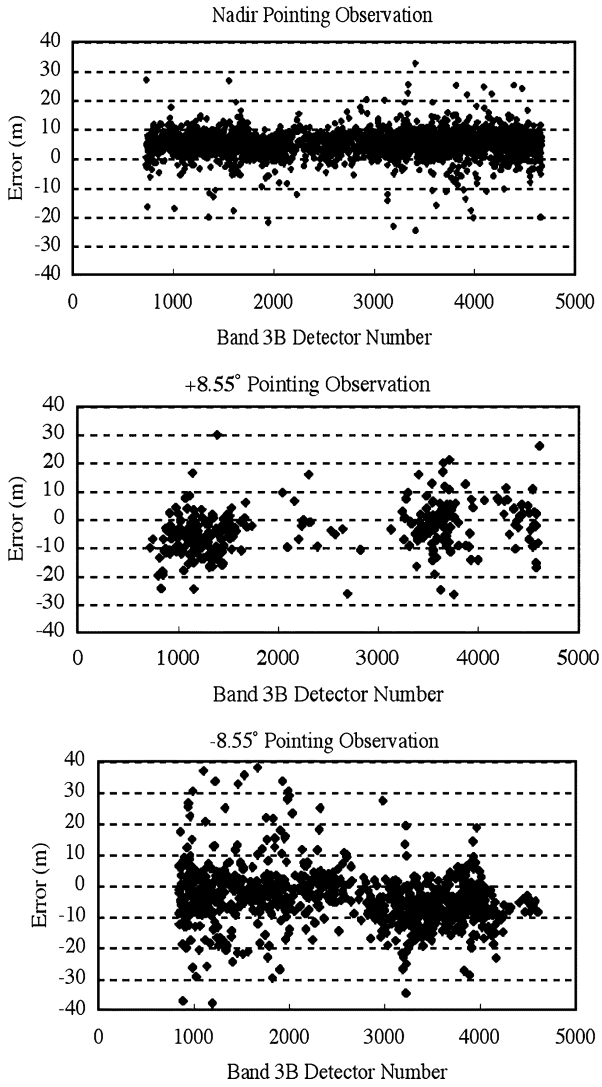

Fig. 4. Band 3B LOS vector calibration accuracy.

2) Input the coarse DEM (GTOPO30) database.
3) Apply the radiometric correction coefficients to the image data.
4) Carry out the first stage image matching using the 1/4 compressed image and calculate the parallax.
5) Carry out the second stage image matching using the 1/2 compressed image and the first stage image matching data and calculate the parallax.
6) Carry out the third stage image matching using the full-resolution image and the second stage image matching data.
7) Generate the ellipsoid base (WGS-84) elevation data (Z data). This process includes the generation of the LOS vectors of detectors for band 3N and 3B expressed by Earth-centered reference (ECR) coordinate frame and the calculation of a tie point of the extended lines of these two LOS vectors.
8) Resample the Z data on a selected map projection.
9) Output the map projected Z data.

The ASTER DEM products were evaluated comprehensively both for the horizontal values (geolocation accuracy) and the

TABLE II
ACCURACY OF DEM DATA

Site Name	Number of GCPs	Pointing Angle (deg)	Average error (m)			σ (m)		
			Longitude	Latitude	Elevation	Longitude	Latitude	Elevation
Tsukuba 1	20	0.02	-8.3	5.1	15.1	5.1	6.6	3.5
Tsukuba 2	20	-0.02	-7.0	8.4	-2.5	12.3	10.4	12.9
Tsukuba 3	20	0.03	8.6	-19.1	-5.5	8.5	4.5	3.7
Tsukuba 4	20	0.03	-4.6	-0.2	-2.4	5.1	4.7	4.2
Tsukuba 5	17	1.58	-31.8	-6.7	-18.2	7.2	7.3	4.5
Tsukuba 6	15	8.59	23.3	-30.8	-0.2	5.6	5.1	5.8
Yatsugatake 1	12	8.59	-11.5	12.9	9.3	12.1	9.0	3.3
Yatsugatake 2	10	8.59	-13.0	-10.8	-15.1	7.4	2.0	3.4
Mt. Fuji	20	2.87	12.8	-17.5	-5.2	5.3	4.7	5.4
Unzen	17	2.87	15.3	-12.9	-10.2	6.6	4.9	3.6
Saga 1	7	0.02	-11.9	10.0	6.8	5.1	5.4	4.8
Saga 2	5	0.02	12.2	6.8	13.0	8.1	4.6	3.2
Saga 3	11	-5.69	20.9	-3.7	2.0	6.5	5.1	2.1
Saga 4	9	-2.87	15.3	-2.5	-4.5	6.8	6.5	2.9
Total	203	---------	0.3	-5.8	-2.2	17.2	13.5	10.0

vertical values (elevation). Two methods were adopted to evaluate the accuracy of the DEM products.

1) Comparison of ASTER DEM data with high-accuracy GCPs. The horizontal and vertical values for each GCP site are measured by a differential type GPS. The accuracies are estimated to be better than ±3.5 m for the horizontal and better than ±1 m for the vertical.
2) Comparison of ASTER DEM Z data to a more accurate DEM database derived from 1/25 000 topographic maps.

A. Comparison of DEM Data With High-Accuracy GCPs

Table II shows the results evaluated through the comparison with high-accuracy GCPs. Only Yatsugatake and Mount Fuji are mountain areas with an elevation higher than 3000 m. The horizontal geolocation accuracy is almost consistent with a reported spacecraft position accuracy of 50 m, which is quite consistent with the accuracy of the calibrated instrument system parameters shown in Fig. 2. The elevation accuracy is 20 m with 95% confidence (2σ), which is quite consistent with the accuracy of the calibrated instrument system parameters shown in Fig. 4.

B. Comparison of DEM With Database

Figs. 5 and 6 show the generated full images of the elevation for Mount Yatsugatake and Tsukuba in Japan and one example of the horizontal profile for each image. An example of the elevation error profile for each image is also shown in these figures. The elevation accuracy is quite consistent with the comparison with high-accuracy GCPs shown in Table II, except for the sharp ups and downs in mountainous areas.

Fig. 7 shows the error histograms for two typical scenes. One is the mountain area (Yatsugatake) with the peak frequency at an

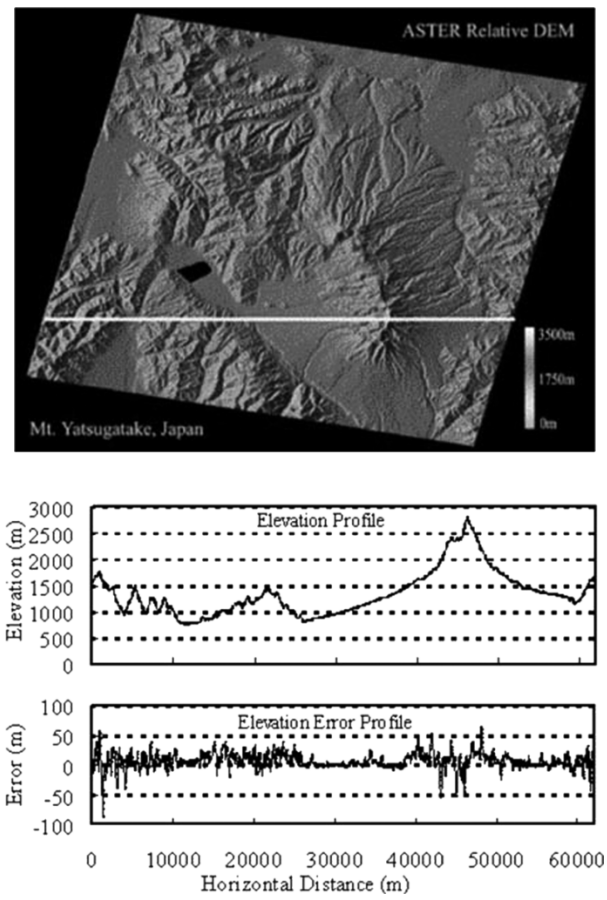

Fig. 5. DEM data of Mount Yatsugatake (a typical mountain area in Japan) and comparison with DEM database. The profiles are data along the white line in the image.

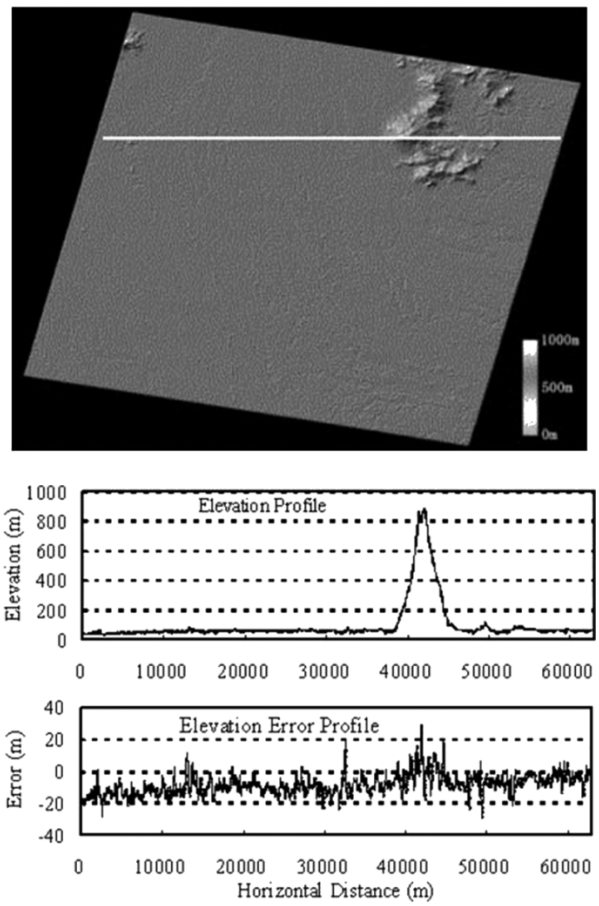

Fig. 6. DEM data of Tsukuba (a typical plane area in Japan) and comparison with DEM database. The profiles are data along the white line in the image.

error of about −10 m. Another is a plain area (Tsukuba) with the peak frequency at an error of about 0 m. These peak frequency errors can be attributed to a combination of the calibration error for the instrument parameters and the spacecraft altitude error. They are considered to be around 10 m.

V. ASTER DEM Data Products—U.S. Version

The U.S. version of the ASTER DEM standard data product is produced on-demand by NASA's Land Processes Distributed Active Archive Center (LP DAAC) at the U.S. Geological Survey (USGS) Earth Resources Observations Systems Data Center using commercial-off-the shelf (COTS) software. The software employs a rigorous mathematical model and uses the satellite ephemeris information from the ASTER Level-1A data to create epipolar images from the 3N and 3B bands. It then applies digital stereo correlation methods to the common area between the 3N and 3B epipolar images, calculating the parallax differences and thus deriving elevation values (Z) for every point (X,Y) in the common image area. The software exports the geolocated elevation data as an HDF-EOS formatted DEM that is archived by the LP DAAC and is available to users via the EOS Data Gateway (EDG).

Two types of ASTER DEMs are produced by the LP DAAC: an *absolute* DEM and a *relative* DEM. The absolute DEM is produced with the aid of user-supplied GCPs, while the relative DEM is produced based on ASTER and spacecraft ephemeris

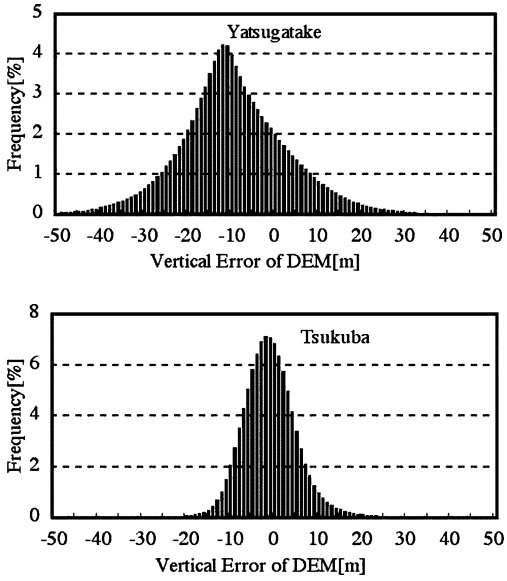

Fig. 7. Error histograms for two typical scenes.

data. As specified by the Algorithm Theoretical Basis Document (ATBD) [5] for ASTER DEMs, the absolute DEM is designed to have an accuracy (RMSExyz) of up to 7 m, depending upon the number and quality of GCPs used in its production. The ATDB cites an accuracy specification for the relative DEM of 10–30 m RMSExyz.

U.S. ASTER DEM products, both the absolute and relative DEMs, are validated standard data products [6]. That is, they have been evaluated and verified to meet the prelaunch specifications set for them in the ASTER DEM ATBD using test sites for which higher resolution DEMs exist and where high-quality GCPs were collected. Discussed here are results from studies conducted at two of those validation sites. One, the Drum Mountains site, is located in west-central Utah and exhibits mountainous terrain typical of the Basin and Range province of the western U.S. The other, the Okoboji site, is located in northwest Iowa and exhibits low, gently rolling terrain typical of the Midwest region of the U.S.

During initial validation studies, GCPs were collected at both sites, and map and aerotriangulation (AT) data were compiled and used as check points where available. GCPs not used in the production of absolute DEMs for these sites were used in the validation process. In addition, data from the USGS National Elevation Dataset (NED) were used as a primary validation standard. Table III summarizes validation statistics derived by subtracting Drum Mountains ASTER DEM elevations from various control elevations.

In all comparisons, the accuracy of the ASTER absolute DEM meets or exceeds prelaunch specifications. Fig. 8 compares shaded-relief images derived from ASTER DEM data and NED data for the Drum Mountains. The black transect lines locate the topographic profiles shown in Fig. 9.

The profiles in Fig. 9 confirm the observation from Table III that ASTER DEM elevations tend to be slightly lower than corresponding NED elevations in the Drum Mountains area. The profiles also show the elevation differences to be more pronounced in areas of high relief.

TABLE III
SUMMARY OF VALIDATION STATISTICS COMPILED FOR THE ABSOLUTE DEM GENERATED FROM ASTER DATA OF THE DRUM MOUNTAINS VALIDATION SITE

Results for the Absolute Drum Mountains DEM (meters)														
GPS GCPs minus DEM						Map & AT Verify Points minus DEM					NED minus DEM			
No. Pts.	Min.	Max.	Mean	RMSE		No. Pts.	Min.	Max.	Mean	RMSE	Min.	Max.	Mean	SD
13	-10.4	18.1	4.44	8.42		44	-13.8	55.7	3.33	13.24	-189	195	4.49	9.34

TABLE IV
SUMMARY OF VALIDATION STATISTICS COMPILED FOR THE ABSOLUTE DEM GENERATED FROM ASTER DATA OF THE OKOBOJI VALIDATION SITE

Results for the Absolute Okoboji DEM (meters)													
GPS GCPs minus DEM					Map Verify Points minus DEM					NED minus DEM			
No. Pts.	Min (m)	Max.	Mean	RMSE	No. Pts.	Min.	Max.	Mean	RMSE	Min.	Max.	Mean	SD
9	-4.0	17.0	2.93	8.34	14	-9.2	16.0	1.03	7.61	-56	182	2.45	11.45

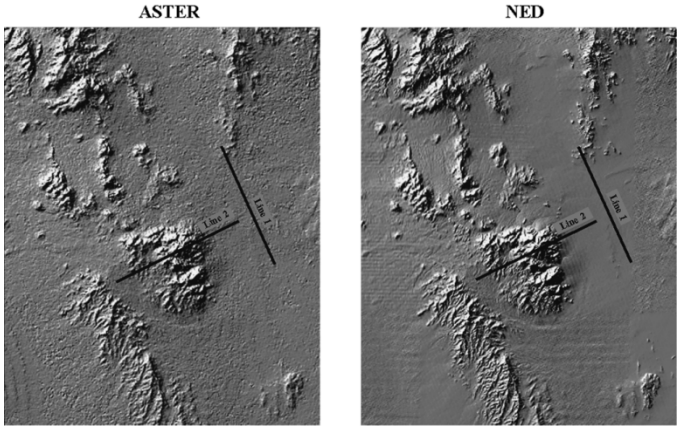

Fig. 8. Drum Mountains site shaded relief images produced from ASTER DEM (absolute) data. Transect lines locate profiles shown in Fig. 9.

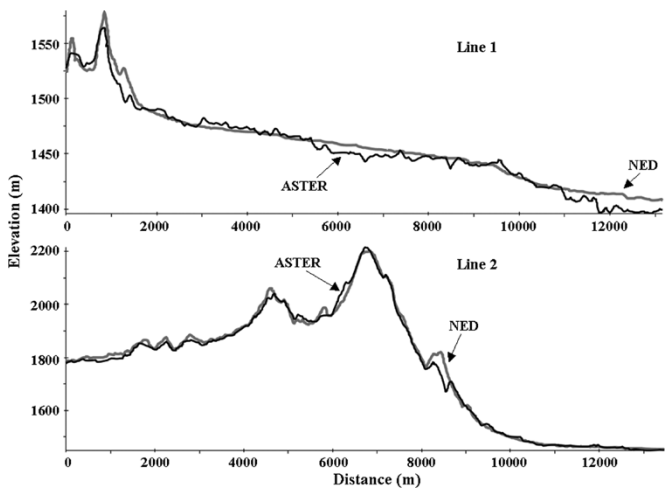

Fig. 9. Drum Mountains topographic profiles. (Black) ASTER DEM profile. (Gray) NED data profile. Elevations and distances are in meters.

Table IV summarizes validation statistics derived by subtracting Okoboji validation site ASTER DEM elevations from various control elevations. In all comparisons, the accuracy of the ASTER absolute DEM meets or exceeds prelaunch specifications.

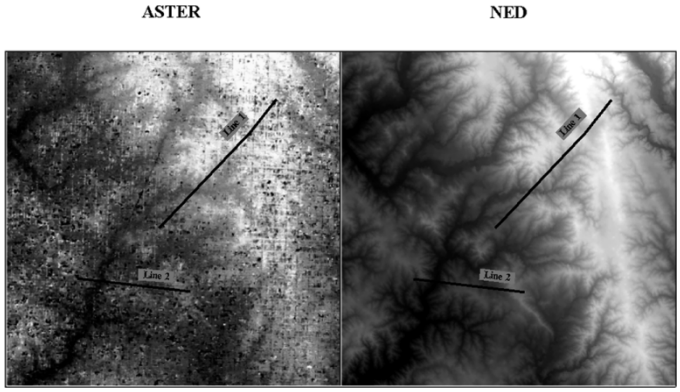

Fig. 10. Okoboji site shaded relief images produced from ASTER DEM (absolute) data and NED data. Transect lines locate profiles shown in Fig. 11.

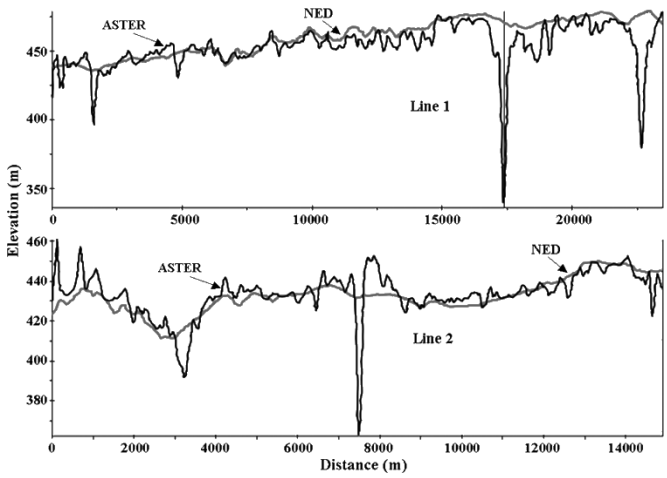

Fig. 11. Okoboji site topographic profiles. (Black) ASTER DEM profile. (Gray) NED data profile. Elevations and distances are in meters.

Fig. 10 compares grayscale images of the ASTER DEM data and NED data for the Okoboji site. The black transect lines locate the topographic profiles shown in Fig. 11. Both figures

TABLE V
SUMMARY OF VALIDATION STATISTICS COMPILED FOR RELATIVE DEMS GENERATED IN 2002 AND 2004 FROM ASTER DATA OF THE DRUM MOUNTAINS AND OKOBOJI VALIDATION SITES

Results for the Drum Mountains and Okoboji Relative DEM (meters)						
	DOQ vs. Orthoimage		NED minus ASTER DEM			
Relative DEM Evaluated	RMSEx	RMSEy	Z Min.	Z Max.	Z Mean	Z Std. Dev.
Drum Mountains – 2002	N/A	N/A	-158	279	6.4	19.7
Drum Mountains – 2004 (2000 scene)	107.6	46.2	-213	188	-17.3	18.3
Drum Mountains – 2004 (2003 scene)	113.1	62.4	-224	211	-6.2	31.2
Drum Mountains – 2004 (2004 scene)	44.6	47.0	-73	215	28.4	31.3
Okoboji - 2002	N/A	N/A	-149	113	0.7	7.7
Okoboji – 2004 (2000 scene)	83.9	7.8	-153	154	-2.2	10.7
Okoboji – 2004 (2003 scene)	57.4	10.2	-363	200	-2.2	17.8

illustrate a somewhat "noiser" ASTER DEM in this lower relief area where image correlation sometimes is more difficult to accomplish.

Relative ASTER DEMs produced at the LP DAAC were not declared validated until a problem discovered with the original version of the production software was fixed, allowing the DAAC production system to generate relative DEMs that met prelaunch accuracy specifications. Subsequent evaluations of relative ASTER DEMs of the Drum Mountains and Okoboji sites generally have shown their accuracies to meet the prelaunch accuracy specifications set for relative DEMs. However, most recent evaluations suggest some degredation in overall accuracy of the relative DEM, possibly related to certain positional inaccuracies in the ASTER metadata caused by incomplete correction of nutation.

Table V compares the accuracies of relative DEMs produced in 2002 with those produced in 2004 for the Drum Mountains and Okoboji validation sites. ASTER DEM elevation accuracies were determined by subtracting the ASTER DEM from NED data for the exact same area. For the evaluations performed in 2004, X-Y accuracies also were calculated by determining the differences in UTM coordinates for the same photo identifiable point (usually road intersections) in the ASTER orthoimage and a USGS digital orthophoto quad.

VI. SUMMARY

The ASTER instrument has an along-track stereoscopic viewing capability. The stereo system configuration, method of parameter adjustment, DEM generation algorithm, and final performance are described in this paper. An important feature of ASTER stereo system concept is the ability to generate DEM data products without referring to GCPs for individual scenes. This is possible because of the excellent spacecraft ephemeris and the instrument parameters. The precise adjustment of these instrument parameters during the initial checkout period is important in order to generate high-quality DEM data.

The vertical accuracy of DEM data was precisely evaluated using high-accuracy GCPs shown in Table II and absolute DEM data shown in Tables III and IV. These results consistently show that the standard deviation is about 10 m, and therefore the vertical accuracy of DEM is about 20 m with 95% confidence (2σ). The horizontal geolocation accuracy appears to be limited by the spacecraft position accuracy which is considered to be better than 50 m.

The accuracy in DEM data indicates that the parameters are well adjusted to have an excellent system performance. In addition, a slight increase in the accuracy was observed for the absolute DEM data generated with referencing GCPs.

ACKNOWLEDGMENT

The authors would like to acknowledge the ASTER Science Team Members for their useful discussion. Work done by M. Abrams was performed at the Jet Propulsion Laboratory, California Institute of Technology, under contract with the National Aeronautics and Space Administration.

REFERENCES

[1] H. Fujisada, F. Sakuma, A. Ono, and M. Kudo, "Design and preflight performance of ASTER instrument protoflight model," *IEEE Trans. Geosci. Remote Sens.*, vol. 36, no. 4, pp. 1152–1160, Jul. 1999.
[2] H. Fujisada, "ASTER Level-1 data processing algorithm," *IEEE Trans. Geosci. Remote Sens.*, vol. 36, no. 4, pp. 1101–1112, Jul. 1999.
[3] A. Iwasaki, H. Fujisada, and M. Torii, "ASTER initial image evaluation," *Proc. SPIE*, vol. 4169, pp. 56–66, 2000.
[4] A. Iwasaki and H. Fujisada, "ASTER geometric performance," *IEEE Trans. Geosci. Remote Sens.*, vol. 43, no. 12, pp. 2700–2706, Dec. 2005.
[5] H. R. Lang and R. Welch, "Algorithm theoretical basis document for ASTER digital elevation models (standard product AST14), Version 3.0," NASA EOS Program, Washington, DC, Alg. Theoret. Basis Doc. ATBD-AST-08, 1999.
[6] G. G. Kelly and G. B. Bailey, "Assessing the characteristics and accuracy of digital elevation data produced from ASTER stereoscopic imagery (abstract)," in *Proc. 14th. Int. Conf. Applied Geologic Remote Sensing Program With Abstracts*, Las Vegas, NV, 2000.

Hiroyuki Fujisada graduated from the University of ElectroCommunication, Tokyo, Japan, in 1962. He joined the Electrotechnical Laboratory in 1962 where he engaged in research on semiconductor sensors and remote sensing system. He received the Doctoral degree in engineering from the Tokyo Institute of Technology in 1979.

He moved to the Remote Sensing Laboratory of Science, University of Tokyo, in 1997, and remained there until 2002. He established the Sensor Information Laboratory Corporation, Amakubo, Japan, in 2002, and is currently President of the company.

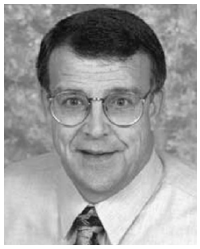

G. Bryan Bailey received the B.A. and M.S. degrees in geology from the University of Iowa, Iowa City, and the Ph.D. degree in mineral exploration from Stanford University, Stanford, CA.

He is currently the Principal Remote Sensing Scientist at the U.S. Geological Survey's (USGS) Earth Resources Observations Systems (EROS) Data Center (EDC), Sioux Falls, SD. He has been employed at EDC since 1978, where he has conducted numerous geologic remote sensing research projects, including studies of China's Qaidam Basin, and has participated as a Lead Instructor in many remote sensing workshops and training courses. From 1990–1999, he served as Project Scientist for the Land Processes Distributed Active Archive Center (LP DAAC) at EDC, during which time he became very knowledgeable about the characteristics and applications of NASA Earth Observing System data. He continues to provide scientific and programmatic liaison between the LP DAAC and the ASTER Science Team and Project. Recently, he was responsible for initiating and leading USGS activities designed to expand and enhance beneficial use of remotely sensed data throughout the USGS. Currently, he is coordinating efforts to revitalize EDC's remote sensing education and training program. He is the author of many scientific publications and other program- and policy-related papers.

Glenn G. Kelly received the B.S. degree in civil engineering from South Dakota State University, Brookings, in 1969.

Upon graduation, he was employed at the National Mapping Division, U.S. Geological Survey. Until 1987, he worked at the Rocky Mountain Mapping Center where he supervised several field mapping projects and the Analytical Aerotriangulation Unit. In 1987, he transferred to the Earth Resources Observations Systems (EROS) Data Center, Sioux Falls, SD. Initially he participated in a number of investigations to develop the application of digital image data to mapping program requirements. For the past several years, he has been involved in projects designed to evaluate a variety of digital cartographic products, particularly digital elevation data products, and to extract from those digital elevation data surface hydrographic features. On January 2, 2004, he retired from the U.S. Geological Survey after nearly 34 years of service.

Seiichi Hara received his degrees from Kagoshima University, Kagoshima, Japan, in 1984 and 1988.

He has been with Central Computer Services Co. Ltd, Tokyo, Japan, since 1988. He is currently a System Engineer.

Michael J. Abrams received his degrees from the California Institute of Technology, Pasadena, in 1970 and 1973.

Since joining the Jet Propulsion Laboratory, Pasadena, CA, in 1973, he has concentrated on applications of remote sensing to geologic studies. His work has included studies related to mineral exploration, ophiolite formation, and volcanic hazards. Currently he is the ASTER Science Team Leader on NASA's EOS Terra project.